NASA TECHNICAL MEMORANDUM

NASA TM X-2591

NASA TM X-2591

EVALUATION OF A SELF-ASPIRATING LOCAL TOTAL ENTHALPY PROBE IN A LOW-DENSITY ARC-HEATED HYPERSONIC WIND TUNNEL

by Robert W. Guy and Andronicos G. Kantsios

Langley Research Center

Hampton, Va. 23365

NATIONAL AERONAUTICS AND SPACE ADMINISTRATION • WASHINGTON, D. C. • AUGUST 1972

1. Report No.	2. Government Accession No.	3. Recipient's Catalog No.
NASA TM X-2591		

4. Title and Subtitle	5. Report Date
EVALUATION OF A SELF-ASPIRATING LOCAL TOTAL ENTHALPY PROBE IN A LOW-DENSITY ARC-HEATED HYPERSONIC WIND TUNNEL	August 1972
	6. Performing Organization Code

7. Author(s)	8. Performing Organization Report No.
Robert W. Guy and Andronicos G. Kantsios	L-8248
	10. Work Unit No. 502-04-03-07
9. Performing Organization Name and Address	11. Contract or Grant No.
NASA Langley Research Center Hampton, Va. 23365	
	13. Type of Report and Period Covered
12. Sponsoring Agency Name and Address	Technical Memorandum
National Aeronautics and Space Administration Washington, D.C. 20546	14. Sponsoring Agency Code

15. Supplementary Notes

16. Abstract

A shock-swallowing, self-aspirating, local total enthalpy probe has been evaluated in a low-density nonequilibrium, hypervelocity airstream. The probe, which incorporated an air gap to separate the internal and external cooling passages, was tested in an electric arc-heated wind tunnel at an average Mach number of 11.7 and an average Reynolds number per meter of 5.7×10^4. The free-stream enthalpy-probe data are compared with bulk calorimeter measurements of total enthalpy at the beginning of the gas expansion and with local total enthalpy inferred from a theoretical nonequilibrium gas expansion model by using free-stream velocity measurements obtained from a mass flow probe. The three techniques are in relative agreement at the lower enthalpies (<4 MJ/kg). However, at the higher enthalpies (>4 MJ/kg), the enthalpy-probe data lie considerably below the other data. This low data may be caused by the chemical and vibrational energy frozen in the flow not being sensed by the probe. Other problems associated with the shock-swallowing total enthalpy probe are discussed in the paper, and recommendations for improving the probe performance are presented.

17. Key Words (Suggested by Author(s))	18. Distribution Statement
Enthalpy probe Arc-tunnel calibration Gas temperature measurements	Unclassified – Unlimited

19. Security Classif. (of this report)	20. Security Classif. (of this page)	21. No. of Pages	22. Price*
Unclassified	Unclassified	22	$3.00

*For sale by the National Technical Information Service, Springfield, Virginia 22151

EVALUATION OF A SELF-ASPIRATING LOCAL TOTAL ENTHALPY PROBE IN A LOW-DENSITY ARC-HEATED HYPERSONIC WIND TUNNEL

By Robert W. Guy and Andronicos G. Kantsios
Langley Research Center

SUMMARY

A shock-swallowing, self-aspirating, local total enthalpy probe has been evaluated in a low-density nonequilibrium, hypervelocity airstream. The probe, which incorporated an air gap to separate the internal and external cooling passages, was tested in an electric arc-heated wind tunnel at an average Mach number of 11.7 and an average Reynolds number per meter of 5.7×10^4. The free-stream enthalpy-probe data are compared with bulk calorimeter measurements of total enthalpy at the beginning of the gas expansion and with local total enthalpy inferred from a theoretical nonequilibrium gas expansion model by using free-stream velocity measurements obtained from a mass flow probe. The three techniques are in relative agreement at the lower enthalpies (<4 MJ/kg). However, at the higher enthalpies (>4 MJ/kg), the enthalpy-probe data lie considerably below the other data. This low data may be caused by the chemical and vibrational energy frozen in the flow not being sensed by the probe. Other problems associated with the shock-swallowing total enthalpy probe are discussed in the paper, and recommendations for improving the probe performance are presented.

INTRODUCTION

The study of orbital and planetary reentry has required development of high-energy wind tunnels which simulate hypervelocity flow conditions over reentry vehicles. One of the major problems associated with such facilities is the measurement of the total enthalpy of the test gas. The measurement techniques fall into two classes: bulk enthalpy measurements and point enthalpy measurements.

Bulk enthalpy measurements are normally used to determine the total energy content of the gas prior to the expansion through the wind-tunnel nozzle or at the test-section entrance, but do not allow determination of local total enthalpy or flow core heat losses. Some of the common bulk enthalpy measurement techniques are thermocouples in the

plenum chamber (ref. 1), energy balance on the facility heater (refs. 2 and 3), the sonic throat technique (refs. 4 to 6), and bulk calorimeters capturing the total tunnel mass flow exhausting from the nozzle throat (refs. 7 and 8).

Point enthalpy measurements are normally used to obtain local total enthalpy in the wind-tunnel test section. Some of the common point enthalpy measurement techniques are total temperature probes (ref. 1), pneumatic probes (ref. 9), stagnation-point heating rate calorimeters (refs. 5 and 6), velocity measurements in highly expanded flows (ref. 10), spectroscopic techniques (ref. 11), and local total enthalpy probes (refs. 12 to 18).

Evaluations of several of these bulk and point total enthalpy measurement techniques may be found in references 3, 8, 19, and 20. Of course, the measurement techniques to be used in a particular wind tunnel depend on the flow environment.

The flow environment of interest in the present investigation was a low-density airstream affected by chemical and vibrational nonequilibrium processes during the expansion through the nozzle. The wind tunnel used was an electric arc-heated facility with a magnetically rotated arc. In this arc tunnel, local test-section measurements of total enthalpy are especially desirable because of the low-density nonequilibrium flow, low arc-heater efficiency, and gas swirl induced by the rotating arc upstream of the tunnel throat. Consequently, a shock-swallowing local total enthalpy probe was designed and evaluated for use in this environment.

In addition to swallowing the shock, the probe design had three other distinguishing features. First, the enthalpy probe was self-aspirating in that the ingested flow was exhausted directly back into the test stream, and thus the need for an external pumping station was eliminated. Second, the coolant channels for the inner and outer probe surfaces were separated by an air gap. And third, the probe inlet design incorporated a balance between the size of the local "point" measurement and the inlet diameter required to capture sufficient energy from the low-density stream to measure temperatures and probe air and coolant flow rates accurately. This balance resulted in an enthalpy probe with an inlet diameter of 1.48 cm, an outer diameter of 3.18 cm, and a length of 38.1 cm.

This paper will discuss the performance of this local total enthalpy probe in a low-density nonequilibrium flow. The probe was tested in a hypervelocity airstream at an average Mach number of 11.7 and an average Reynolds number of 5.7×10^4 per meter over a total enthalpy range (based on bulk calorimeter measurements) of 1.48 to 8.75 MJ/kg. The enthalpy-probe data are compared with bulk calorimeter measurements obtained at the beginning of the nozzle expansion and with point total enthalpy measurements inferred by using free-stream velocity measurements from a mass flow probe together with a nonequilibrium gas expansion model.

SYMBOLS

A	area
B	constant in equation (3)
C_D	discharge coefficient
C_p	specific heat at constant pressure
c	constant in equation (3)
d	inner diameter
H	enthalpy
K	constant in equation (6)
M	Mach number
$\dot{m}$	mass flow rate
N_{Re}	unit Reynolds number, $\rho V/\mu$
p	pressure
R	specific gas constant
T	temperature
ΔT	coolant temperature rise
t	time
V	velocity
γ	ratio of specific heats
λ	mean free path length

μ	dynamic viscosity
ρ	mass density

Subscripts:

a	airflow
actual	actual (measured) flow
cal	bulk calorimeter
e	exhaust
f	frozen
i	inlet
ideal	ideal (calculated) flow
p	probe
t	stagnation condition anywhere in gas expansion
th	wind-tunnel throat
t,1	stagnation condition at beginning of gas expansion
t,2	stagnation condition behind a normal shock in free stream
w	coolant
1	static condition upstream of enthalpy-probe orifice
∞	free-stream static condition; in the case of temperature, the reference is to translational and rotational temperature

Superscript:

*	enthalpy-probe rounded-orifice throat

APPARATUS AND TESTS

Tunnel and Test Conditions

The facility used in the evaluation of the enthalpy probe was the Langley 30.5-cm hypersonic arc tunnel (fig. 1) with air as the test gas. The tunnel is described in reference 8. Briefly, the air is heated by a magnetically rotated electric arc and expanded through a 5.38-mm-diameter circular-arc throat and a 5° half-angle conical nozzle to a 30.5-cm-diameter closed-jet test section. A five-stage steam ejector provides vacuum for continuous tunnel operation. A range of enthalpies is obtained by varying the electrode arc gap with different diameter outer electrodes and by injecting selected flow rates of room-temperature air downstream of the plenum chamber.

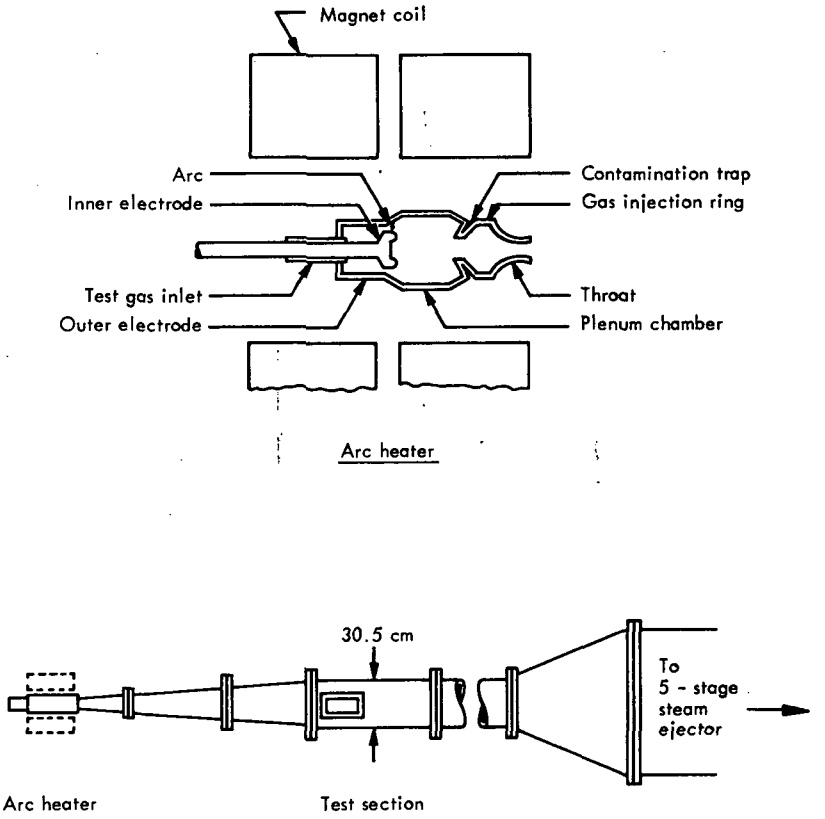

Figure 1.- Schematic drawing of the Langley 30.5-cm hypersonic arc tunnel.

The measured and calculated test parameters for the enthalpy-probe evaluation tests are presented in table I. The total enthalpies listed in this table are bulk calorimeter measurements representing the enthalpy at the entrance to the tunnel throat region. Free-stream properties were calculated by use of the Cornell chemical nonequilibrium gas expansion computer program (ref. 21) which had been modified to account approximately

for vibrational nonequilibrium (ref. 8). The free-stream properties were obtained from this program at measured values of stream pitot pressure.

TABLE I.- ARC-TUNNEL TEST CONDITIONS

Test	$p_{t,1}$, N/m^2	$H_{t,1}$, MJ/kg	$T_{t,1}$, K	M_∞	p_∞, N/m^2	ρ_∞, kg/m^3	T_∞, K	V_∞, m/sec	$N_{Re,\infty}/m$	λ_∞, cm	$p_{t,2}$, N/m^2
1	4.07×10^5	1.48	1450	11.6	3.54	2.35×10^{-4}	53	1690	11.62×10^4	0.015	618
2	4.68	2.14	1880	11.6	4.11	2.01	71	1960	8.16	.021	709
3	5.41	2.89	2430	11.8	4.34	1.73	87	2200	6.35	.028	774
4	6.34	3.16	2630	11.6	4.96	1.68	103	2360	5.58	.031	864
5	6.31	3.26	2650	11.5	5.23	1.73	106	2370	5.61	.031	896
6	7.04	3.72	2930	11.7	5.11	1.56	113	2520	4.98	.035	909
7	7.49	5.26	3640	11.5	6.47	1.44	151	2900	4.05	.043	1110
8	9.05	7.45	4370	11.9	6.96	1.29	172	3310	3.65	.049	1290
9	8.49	7.77	4450	11.9	6.88	1.24	175	3350	3.51	.051	1270
10	8.75	8.75	4700	11.9	7.24	1.23	182	3460	3.49	.052	1360

Enthalpy Probe

The local total enthalpy probe (fig. 2) was a water-cooled copper calorimeter with separate cooling passages for the external and internal (calorimeter) parts of the probe. A 0.75-mm air gap separated the external and internal coolant passages to minimize heat transfer from one to the other. The air gap extended to the probe tip and thus allowed minimum external heat transfer to the calorimeter surface in this high external heat-transfer region.

The section of the probe containing the rounded orifice for the measurement of mass flow rate was an integral part of the calorimetric section of the enthalpy probe. This mass flow measuring section was exposed to the external stream at the rear of the probe for a distance of 3.18 cm. An approximate analysis indicated that the extraneous heat gained by this exposure to the external flow was less than 3 percent of that flowing through the calorimetric section of the probe. This extraneous heat input would be offset to some extent by conduction along the stainless-steel pressure tubing and thermocouple sheath which were connected to this section. In addition, the air-out and calorimeter water-out temperatures were measured just upstream of the orifice. Therefore, the small amounts of heat transfer to or from the orifice section were neglected.

The sharp conical inlet (30^o exterior angle) was designed to swallow the shock; thereby, the maximum gas mass flow intake from the low-density airstream was allowed.

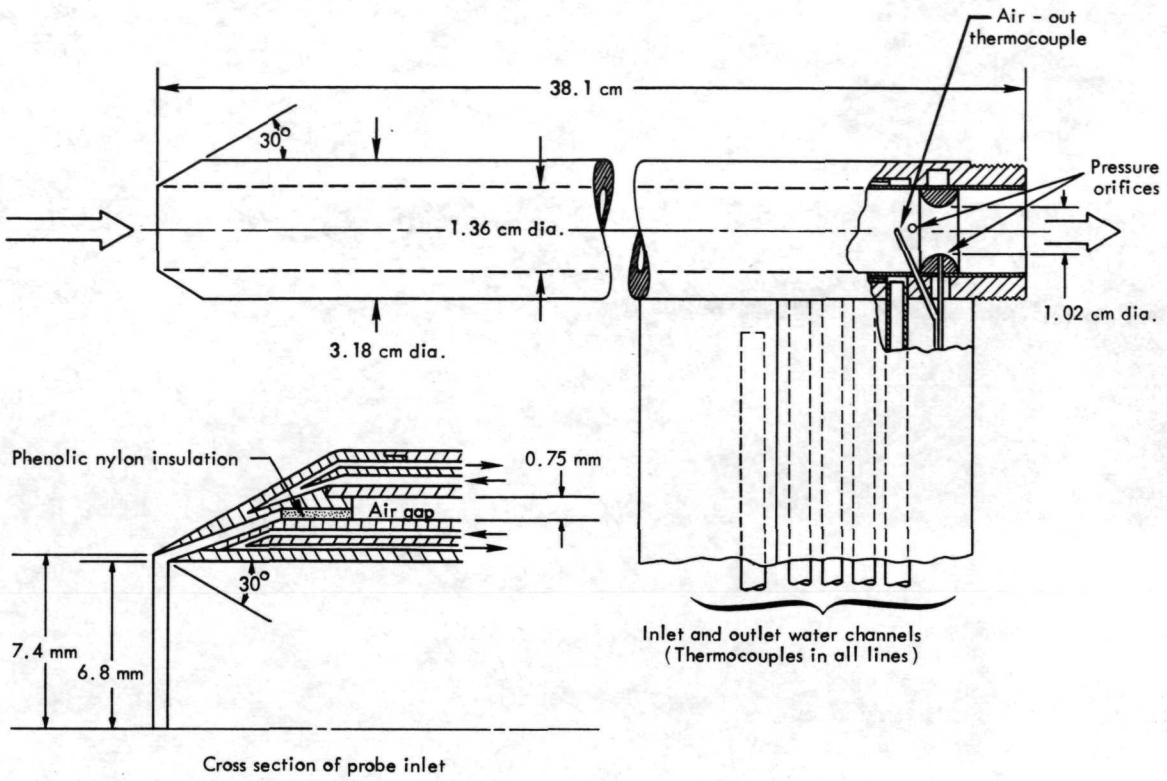

(a) Schematic of probe.

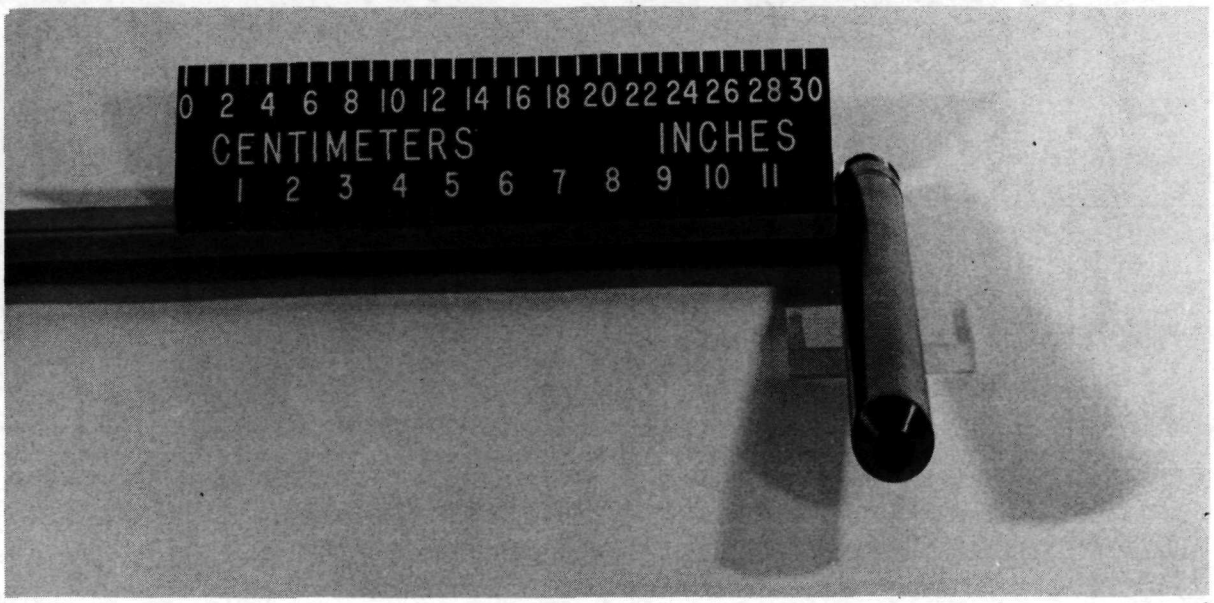

L-70-3948

(b) Front view of probe.

Figure 2.- Shock-swallowing self-aspirating enthalpy probe.

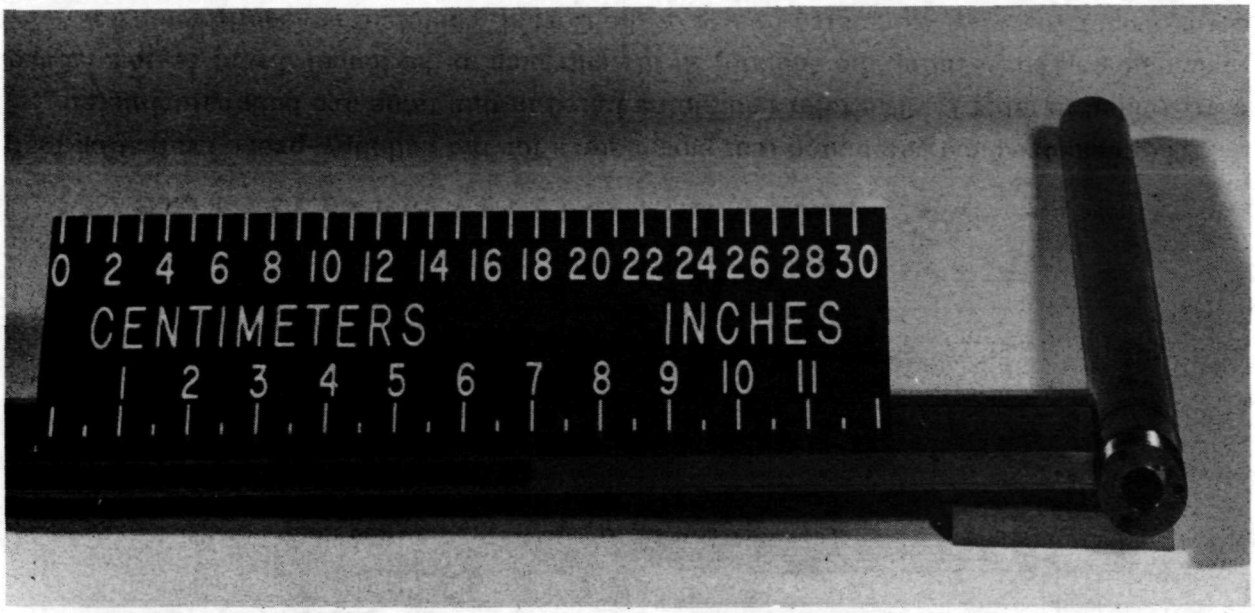

L-70-3949

(c) Rear view of probe.

Figure 2.- Concluded.

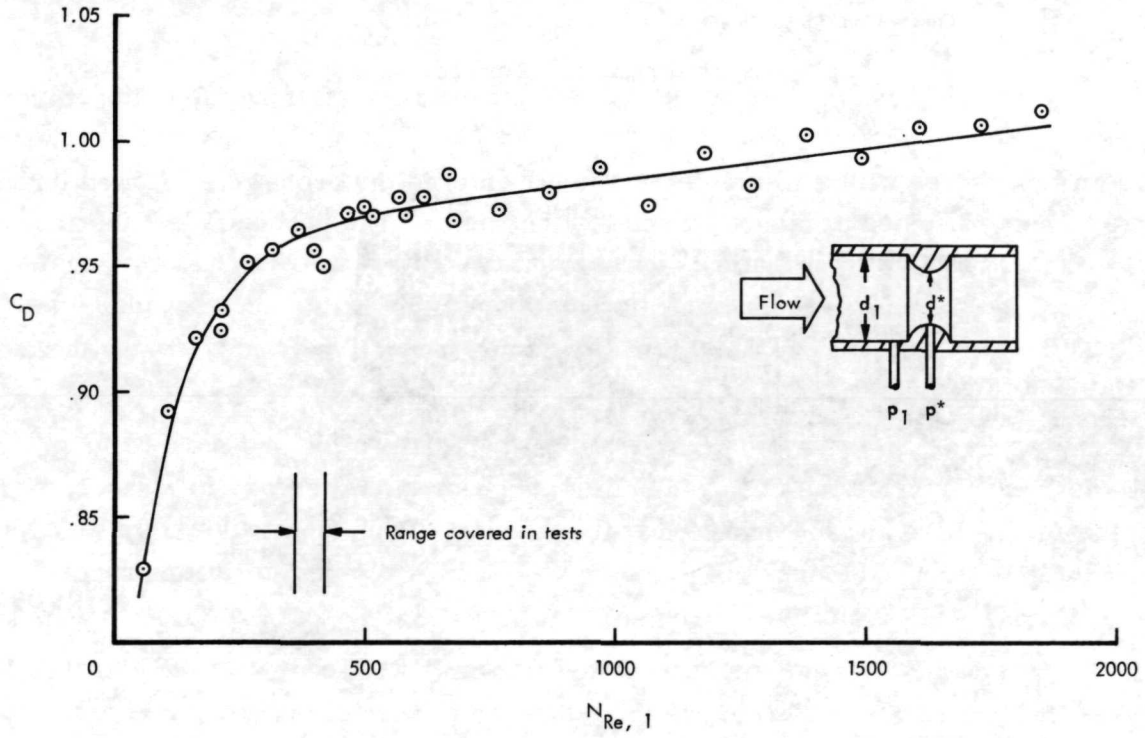

Figure 3.- Calibration of enthalpy-probe rounded orifice. $d_1 = 1.36$ cm; $d^* = 1.02$ cm;

$$N_{Re,1} = \frac{\rho_1 V_1 d_1}{\mu_1} = \frac{4}{\pi} \frac{\dot{m}_{a,p}}{\mu_1 d_1}.$$

The mass flow rate was measured with the orifice installed in the exit of the calorimetric section of the probe. The gas flowing through the probe was exhausted back into the test stream; this self-aspirating design feature used the pumping capacity of the facility and eliminated the need for an external pumping station. Gas mass flow rates through the probe ranged from 0.074 to 0.093 g/sec.

The enthalpy-probe rounded-orifice calibration is shown in figure 3, where the discharge coefficient is presented as a function of probe Reynolds number. The discharge coefficient is defined as

$$C_D = \frac{\dot{m}_{actual}}{\dot{m}_{ideal}} \tag{1}$$

where

$$\dot{m}_{ideal} = \frac{A^* p^* \sqrt{\frac{2}{RT_1}\left(\frac{\gamma}{\gamma - 1}\right)\left(\frac{p_1}{p^*}\right)^{\frac{\gamma-1}{\gamma}}\left[\left(\frac{p_1}{p^*}\right)^{\frac{\gamma-1}{\gamma}} - 1\right]}}{\sqrt{1 - \left(\frac{A^*}{A_1}\right)^2\left(\frac{p^*}{p_1}\right)^{2/\gamma}}} \tag{2}$$

(ref. 22) and where $\dot{m}_{actual}$ was determined by calibration. During the calibration the probe was mounted in the facility. The mass flow rate of the room-temperature calibration air was measured with a rotameter. The air entered the probe inlet, flowed through the orifice, and exhausted to the evacuated test chamber. The probe air-out thermocouple indicated that the air temperature approaching the orifice was 290 K. The highest average temperature across the probe calorimeter exit during the actual enthalpy tests was 360 K; this difference from the calibration temperature is corrected for by the temperature term in equation (2).

The flow across the rounded orifice was not sonic since the pressure ratio p^*/p_1 was greater than the value for a choked orifice; thus, it was necessary to measure both the upstream pressure and the orifice throat pressure. Probe mass flow rate was determined from the measured values of p_1, p^*, T_1, and A^* by an iteration process involving equations (1) and (2) and figure 3.

A 30-gage swaged copper-constantan thermocouple was located at the entrance and exit of each cooling channel to measure the temperature rise of the cooling water. A 36-gage swaged copper-constantan thermocouple was located on the probe center line at the rear of the calorimeter tube to measure the temperature of the exhaust gas. The thermocouple calibrations were referenceable to the National Bureau of Standards calibrations.

The probe coolant was helium-pressurized distilled water. Coolant flow rates were measured with turbine flowmeters and ranged from 1.76 to 4.13 g/sec.

Because of the low density of the flow, the inner diameter of the enthalpy probe was made sufficiently large (1.36 cm) to insure the collection of an adequate gas mass flow to provide a cooling water temperature rise of 10 K or greater. The probe was made relatively long (38.1 cm) so that the gas temperature at the orifice would not be significantly greater than the temperature at which the orifice was calibrated.

The times required for the probe measurements to reach steady-state levels were very long, especially at the lower enthalpies. Evidently, the large mass of the probe calorimeter surface and the orifice section combined with the low flow density caused the poor response.

Mass Flow Probe

The water-cooled mass flow probe is described in reference 8 and is shown schematically in figure 4. Based on results from reference 23, the probe inlet was designed with equal interior and exterior angles of 30° so that the capture area would be equal to the geometric inlet area. The remainder of the probe was designed to minimize pressure losses so that the shock would be swallowed. The 6.12-mm-diameter inlet was followed by a 6.35-mm-long constant-area section with a length-diameter ratio of 1.22, an expansion region to a 1.092-cm constant-area section 50 cm long, a 50-cm length of plastic vacuum tubing, a 4.75-mm-diameter calibrated corner-tap orifice, and a quarter-turn ball valve.

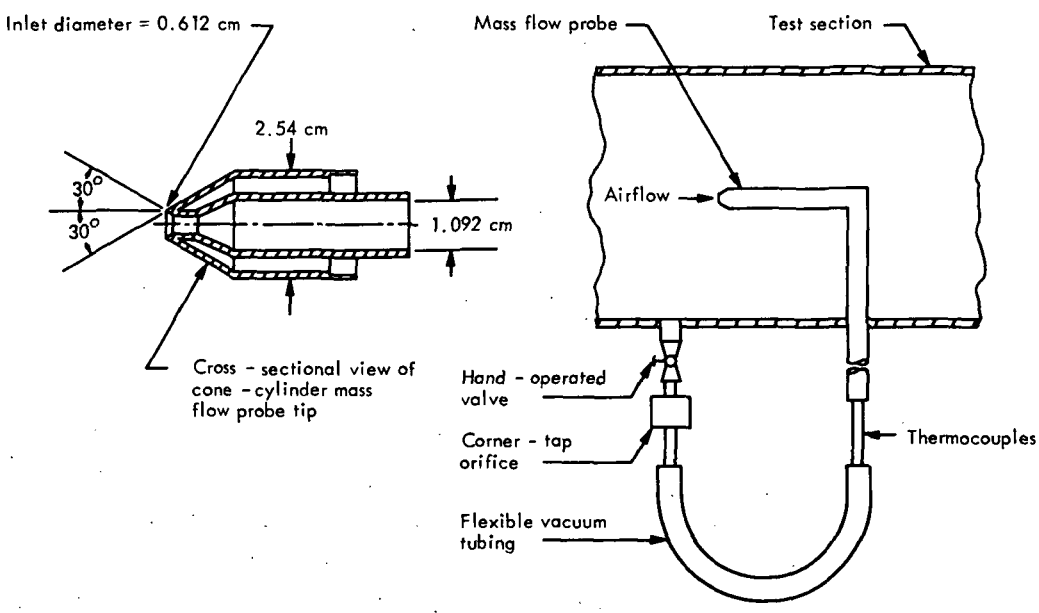

Figure 4.- Schematic drawing of shock-swallowing mass flow probe.

Copper-constantan thermocouples located upstream of the orifice indicated that the test gas had cooled to room temperature prior to flowing through the orifice. Flow through the probe was exhausted back into the test stream slightly ahead of the probe tip, and thus the need for an external pumping station was eliminated.

Measurements of pressure drop through the probe during the orifice calibration indicated that the shock should be swallowed during the tests. Shock swallowing was confirmed from photographs (fig. 5) showing that the hot gas cap on the probe tip disappeared when flow was allowed to pass through the mass flow probe.

With flow through the probe, mass flow rate was measured; with no flow through the probe, pitot pressure was measured. These two measurements were used to calculate local velocity.

Bulk Calorimeter

A schematic of the bulk calorimeter is presented in figure 6 and a discussion of this device may be found in reference 8. The outer wall of the calorimeter was coiled copper tubing sealed with soft solder. The calorimeter inlet adjoining the wind-tunnel throat had a 7.6-cm inner diameter and was 12.7 cm long. A converging section 7.6 cm long was followed by the calorimeter exit section which had a 3.8-cm inner diameter and was 30.5 cm long. A calorimeter insert (fig. 6) was used to absorb more heat from the air. This insert consisted of 3.75-cm-diameter copper disks mounted along a 30.5-cm length of 1.9-cm-diameter copper tube. Holes with diameters of 6.35 mm were drilled in the disks, and the disks were mounted on the copper tube so that the flow could not pass straight through the calorimeter.

Measurements were made with the following instrumentation: iron-constantan thermocouples for the inlet and outlet water temperatures, a lateral series of chromel-alumel thermocouples for the exhaust gas temperature, a turbine flowmeter for calorimeter cooling water flow rate, and the facility corner-tap orifice for measuring air mass flow rate through the bulk calorimeter.

DATA REDUCTION

Enthalpy Probe

At the lower enthalpies, the time required for the probe water and air-out temperature measurements to reach steady-state levels exceeded the available tunnel test time which was controlled by the temperature limit on the arc-heater magnetic coil (fig. 1). Therefore, to determine the steady-state total enthalpy, an exponential equation,

$$H_{t,p} = H(t)_p + Be^{-ct} \tag{3}$$

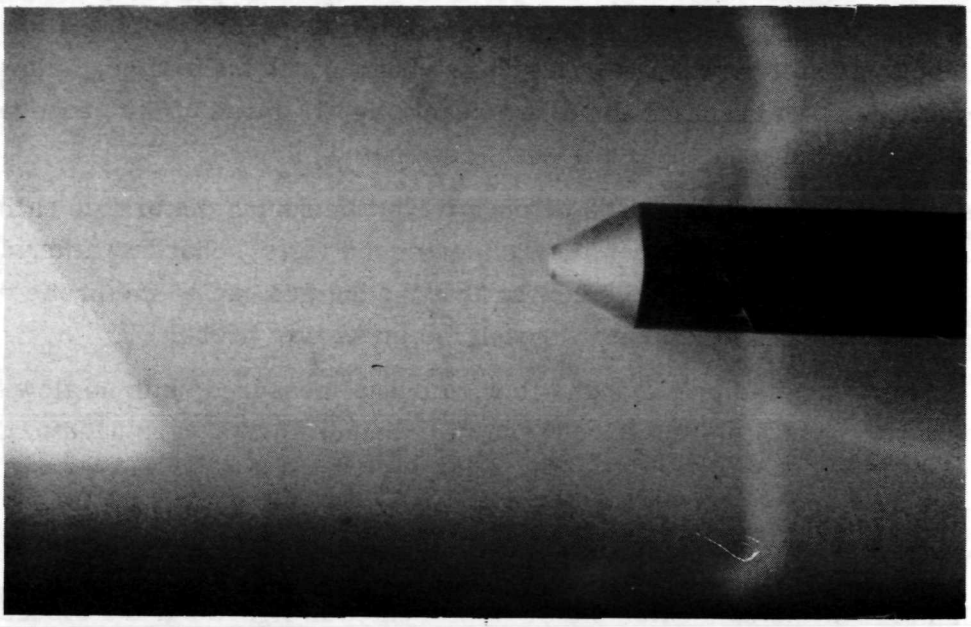

(a) Valve open.

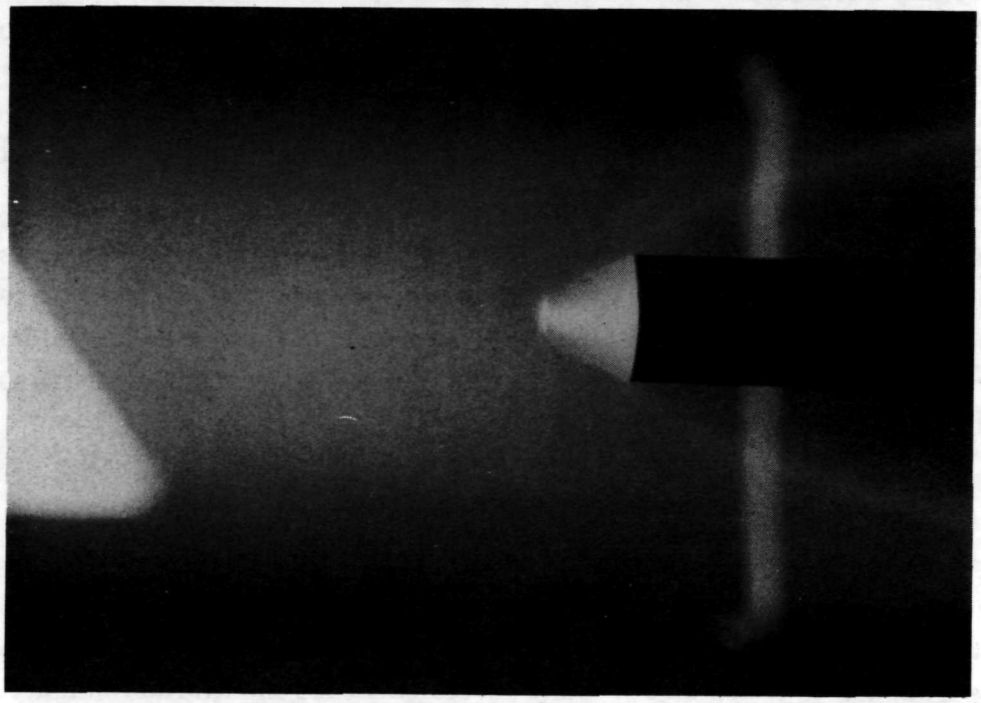

L-72-2454

(b) Valve closed.

Figure 5.- Mass flow probe tip showing swallowing of shock when flow is pumped through probe and stagnation region gas cap when there is no flow through probe.

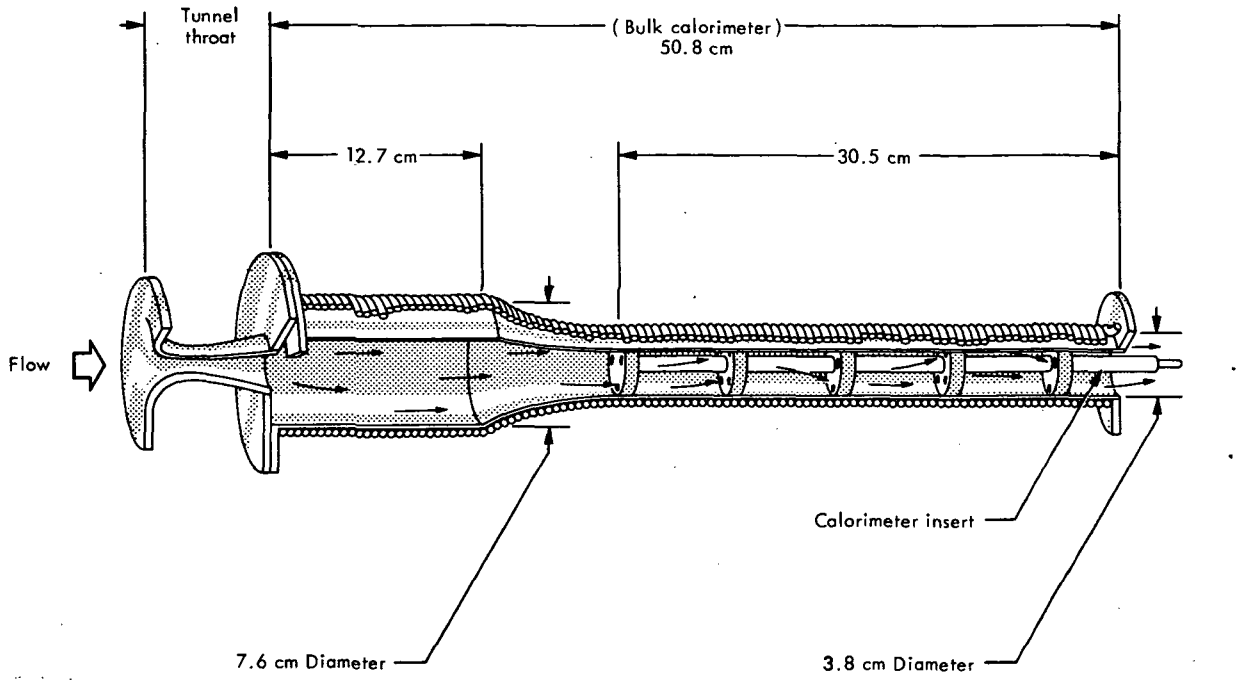

Figure 6.- Schematic drawing of bulk calorimeter attached to tunnel throat.

was fitted to each set of transient data which did not reach a steady-state level. The test times were sufficiently long (at least 180 seconds) to obtain enough data for this extrapolation. The transient enthalpy, $H(t)_p$ in equation (3), indicated by the probe was calculated at various times from the following heat balance equation:

$$H(t)_p = \frac{\left[\dot{m}_w C_{p,w} \Delta T(t)_w\right]_p}{\dot{m}_{a,p}} + \left[C_{p,a,e} T(t)_{a,e}\right]_p + H_{f,p,e} \qquad (4)$$

The term $H_{f,p,e}$ represents any energy (chemical or vibrational) that may have remained frozen during the passage of the gas through the enthalpy probe. Evaluation of this term would require extensive chemical kinetic calculations involving the low-density, $p_p = O(10^3\ N/m^2)$, internal flow. The term $H_{f,p,e}$ was neglected in the extrapolations of the transient data since it is a constant for a particular test. The possible effects of frozen chemical and vibrational energy on the enthalpy-probe results are discussed in the section "Results and Discussion."

Three typical time histories of the enthalpy-probe response are shown in figure 7. The curves through each set of data represent equation (3) with B and c calculated for that set of data. The accuracy of this equation was confirmed by its successful application to data where the probe did reach steady-state levels during the available test time.

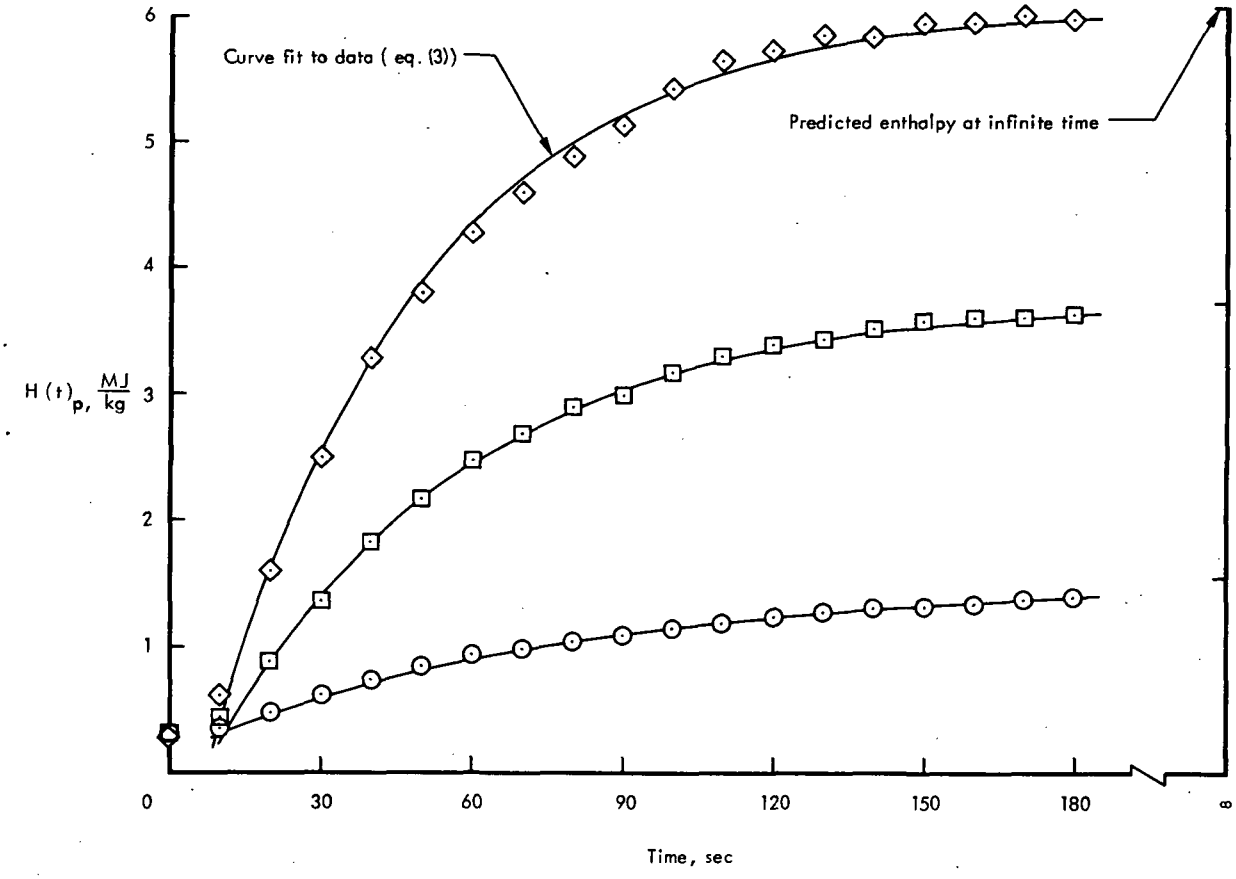

Figure 7.- Probe response at various enthalpy levels.

The mass flow rate through the enthalpy probe was compared with predictions of this flow rate using the enthalpy-probe inlet area together with $\rho_\infty V_\infty$ from mass flow probe results and from the theoretical nonequilibrium gas expansion. The prediction techniques were in relative agreement; however, the measured mass flow rates through the enthalpy probe were greater than the predictions by an average of 28 percent. This difference indicated that the shock was swallowed and that the probe capture area was larger than the geometric inlet area, that is, supercapture (ref. 23). The enthalpy probe was not used as a mass flow probe; therefore, the supercapture was beneficial since the larger capture area caused a greater cooling water temperature rise.

The same inlet design that was used on the mass flow probe (designed to capture a streamtube area equal to the geometric inlet area) was attempted on the enthalpy probe (see fig. 2); however, the air gap at the tip apparently did not act to form the 30° internal angle, and thereby allowed supercapture. This result indicates that errors may be experienced in using the present type of enthalpy probe as a mass flow probe (that is, to determine ρ_∞, V_∞, or $\rho_\infty V_\infty$); however, supercapture introduces no error when the probe is used as an enthalpy probe.

A random-error analysis (ref. 24) was made of the enthalpy-probe data. The analysis showed a standard deviation of 8 percent and a maximum uncertainty of 19 percent on the measured enthalpies.

Mass Flow Probe

Probe mass flow rate and pitot pressure data were obtained with the mass flow probe. The probe was designed, by following the criteria of reference 23, to swallow the shock and capture a streamtube area equal to the geometric inlet area so that

$$\dot{m}_{a,p} = \rho_\infty V_\infty A_{p,i} \tag{5}$$

In hypersonic flow, the pitot pressure is closely approximated by the product of free-stream density and free-stream velocity squared, that is,

$$p_{t,2} = K\rho_\infty V_\infty^2 \tag{6}$$

Since the free-stream flow was in a nonequilibrium state, a value of 0.925 was used for K (ref. 8); however, K would vary no more than 3 percent even if equilibrium flow were assumed. Equations (5) and (6) may be combined to give the local free-stream velocity. Thus,

$$V_\infty = 1.082 \frac{p_{t,2} A_{p,i}}{\dot{m}_{a,p}} \tag{7}$$

In frozen or nonequilibrium hypersonic flow, a significant amount of energy may not be converted to kinetic energy during the gas expansion through the arc-tunnel nozzle. If, in such cases, velocity measurements are to be used to infer local total enthalpy, a model for the gas expansion (frozen or nonequilibrium) must be assumed. In the present study, the Cornell chemical nonequilibrium gas expansion program (ref. 21) was modified to account approximately for vibrational nonequilibrium (ref. 8) and was used to generate a curve of free-stream velocity against total (stagnation) enthalpy at the beginning of the nozzle expansion (fig. 8). The experimental values of velocity were then used to determine total enthalpy from this curve.

A random-error analysis of the velocity data (ref. 24) indicated a standard deviation of 4 percent and a maximum uncertainty of 12 percent. The error in the inferred total enthalpy is not quoted since it is dependent upon the assumed gas expansion model.

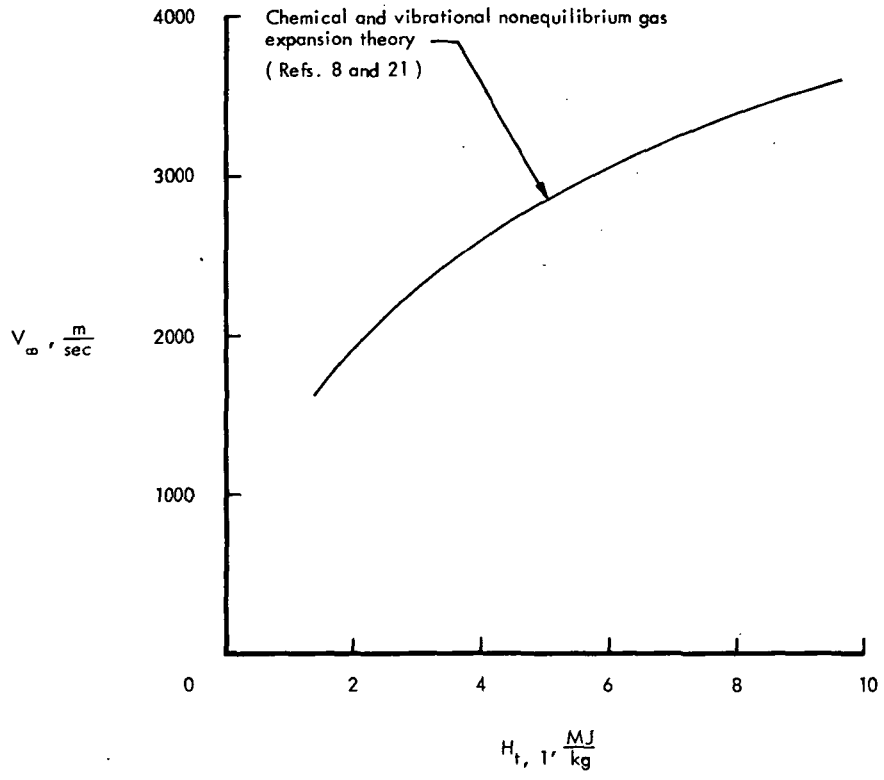

Figure 8.- Nonequilibrium free-stream velocity as a function of total enthalpy at beginning of gas expansion. Other stream properties are given in table I.

Bulk Calorimeter

Total enthalpy at the beginning of the gas expansion was determined (from measurements) by adding the energy absorbed by the throat, that absorbed by the bulk calorimeter, and the residual energy exhausting from the calorimeter; that is,

$$H_{t,cal} = \frac{\left(\dot{m}_w C_{p,w}\,\Delta T_w\right)_{th} + \left(\dot{m}_w C_{p,w}\,\Delta T_w\right)_{cal}}{\dot{m}_a} + \left(C_{p,a,e} T_{a,e}\right)_{cal} \tag{8}$$

No term is included in this equation for frozen energy since the pressure level at which the bulk calorimeter was operated, $p_{cal} = O(10^5\ N/m^2)$, was high enough to allow most dissociated species to recombine in the calorimeter. A random-error analysis of the bulk calorimeter data (ref. 24) indicated a standard deviation of 6 percent and a maximum uncertainty of 15 percent.

RESULTS AND DISCUSSION

Figure 9 is a comparison of total enthalpy as determined from the enthalpy probe, the bulk calorimeter, and the velocity measurements. The abscissa is total enthalpy

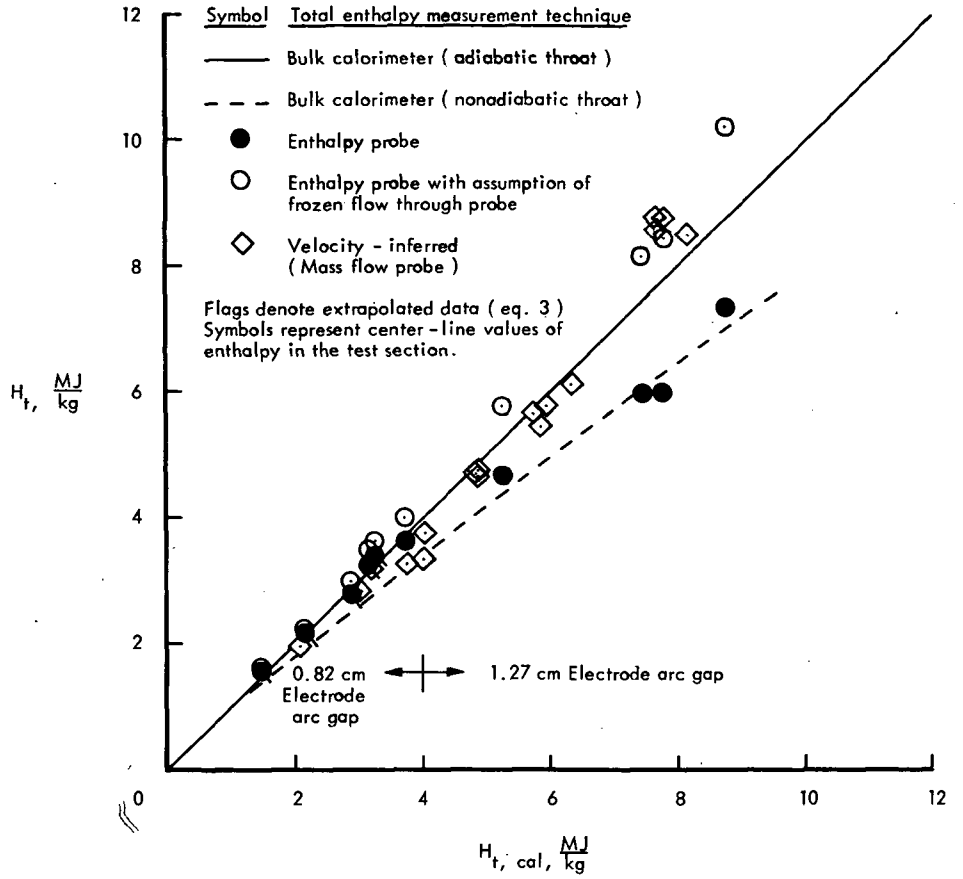

Figure 9.- Comparison of total enthalpy measurements.

measured by the bulk calorimeter, adiabatic flow from the entrance to the throat section of the arc tunnel being assumed (eq. (8)). This total enthalpy at the beginning of the expansion is used as a reference because it is more reliable (nonequilibrium effects are eliminated) than test-section local enthalpy and because the two will be equal if the gas expansion through the nozzle is adiabatic. The ordinate of figure 9 is total enthalpy determined by the techniques mentioned. The solid line represents perfect agreement with the bulk calorimeter measurements of enthalpy prior to the expansion of the gas. The dashed curve represents the total enthalpy in the test section if the gas expansion through the tunnel throat is nonadiabatic, that is, no inviscid core exists in the throat region and any energy lost to the throat cooling water is assumed to be lost from the downstream inviscid core. (See ref. 5.)

The velocity-inferred local total enthalpy data on the tunnel center line are high compared with the bulk calorimeter data at the highest enthalpy level (≈7.7 MJ/kg). Generally, however, the velocity-inferred data support the bulk calorimeter data with the assumption of adiabatic flow from the plenum chamber.

The enthalpy-probe data measured on the tunnel center line are shown in figure 9 by the shaded circular symbols. The flagged symbols indicate tests where equation (3) was used to obtain the steady-state total enthalpy. Data below an enthalpy of 4 MJ/kg were taken with a 0.82-cm electrode arc gap whereas data above 4 MJ/kg were taken with a 1.27-cm electrode arc gap.

The enthalpy-probe data agree well with the bulk calorimeter data (adiabatic flow from the beginning of the gas expansion being assumed) below an enthalpy of 4 MJ/kg. However, above this enthalpy, the probe data fall below the line of perfect agreement and, in fact, agree very closely with the dashed curve for nonadiabatic flow through the throat region. The possibility of nonadiabatic flow through the nozzle throat must be considered (ref. 5) since flow swirl increased significantly (ref. 8) with the outer electrode which was used to obtain the data above 4 MJ/kg. This difference between the enthalpy-probe data and the total enthalpy at the beginning of the gas expansion is more likely to be caused by nonequilibrium processes in the low-density airstream, since the amounts of dissociated species increase significantly at the higher enthalpies. Approximate calculations of chemical recombination (ref. 25) and vibrational relaxation times (ref. 8) indicate that the chemical energy may remain frozen during the passage through the probe whereas the vibrational energy may be released. For example, at 8.75 MJ/kg, the residence time of a gas particle in the probe (a normal shock standing just inside the inlet being assumed) is on the order of 1 millisecond whereas the time required for the recombination of atomic oxygen is on the order of seconds and the vibration relaxation time for diatomic nitrogen is less than a millisecond. These results may also be obtained from the vibrational relaxation times and oxygen recombination times shown graphically in reference 5.

With only the approximate calculations and without a knowledge of lateral diffusion rates or probe and thermocouple catalytic efficiencies, only the limits of the effects of frozen energy on the enthalpy-probe data can be determined. Figure 10 shows, as a function of total energy at the beginning of the arc-tunnel expansion, the amount of energy (chemical and vibrational) that the nonequilibrium gas expansion program (ref. 8) indicates is frozen in the free stream. The open circular symbols in figure 9 were calculated by assuming that $H_{f,p}$ in equation (4) was equal to the total frozen energy entering the enthalpy probe; that is, no frozen energy was released as the gas passed through the probe. With this assumption, $\dot{m}_{a,p}$ and $C_{p,a,e}$ (eq. (4)) also had to be adjusted since the chemical composition of the frozen gas was different from that of room-temperature air. The assumption of frozen flow through the probe has an increasingly large effect on the enthalpy-probe data at the higher enthalpies (fig. 9), and the data with the assumed $H_{f,p}$ added to the probe measurements now lie above the line of perfect agreement. One would expect this result if some of the frozen energy entering the enthalpy probe did recombine (or relax).

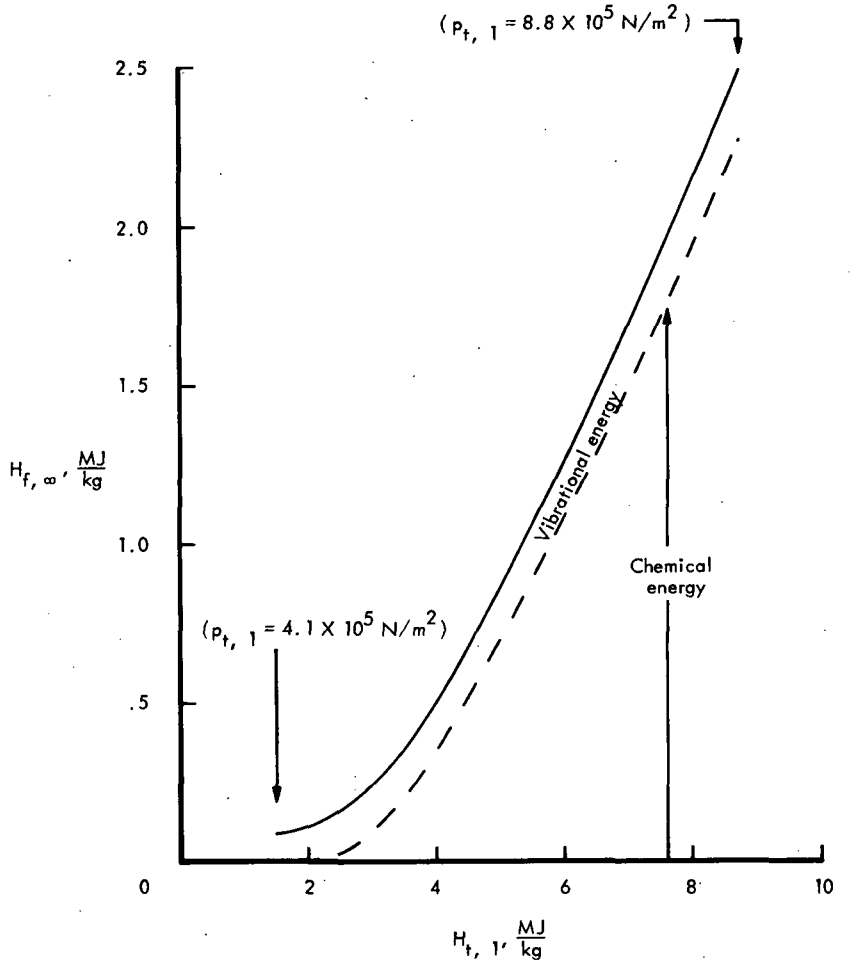

Figure 10.- Calculated frozen energy in test stream of the Langley 30.5-cm hypersonic arc tunnel.

The relatively good agreement of the enthalpy-probe data with the other two methods (fig. 9) at the lower enthalpies tends to prove the probe performance and lends confidence to the enthalpy-probe mass flow rate measurements (where evidence of supercapture was noted). However, several recommendations can be made concerning the probe, some of which will improve its performance. First, this type of probe (with the air gap extending to the tip) does not perform well as a mass flow probe in low-density flow. Second, the diameter and length of the probe could be reduced somewhat without affecting the probe accuracy significantly; this reduction should improve probe time response. Third, the orifice section should be isolated as much as possible from the calorimeter section of the probe in order to improve probe time response and remove any extraneous heat sources or sinks (although these are believed to be small even with the present design). Fourth, mass flow rate calibrations using heated air (to temperatures expected during the tests) would lend still more confidence to the probe measurements of enthalpy. And fifth, a

knowledge of the chemistry of the exiting flow is needed and, in this regard, determination of the catalytic efficiency of the air-out thermocouple surface would be helpful.

CONCLUDING REMARKS

A shock-swallowing, self-aspirating, local total enthalpy probe has been evaluated and compared with two other measurement techniques in a low-density nonequilibrium, hypervelocity airstream at an average Mach number of 11.7 and an average Reynolds number per meter of 5.7×10^4. Generally, total enthalpies inferred from a nonequilibrium gas expansion model using free-stream velocity measurements from a mass flow probe agreed with bulk calorimeter total enthalpy when an adiabatic expansion through the arc-tunnel nozzle was assumed. At the lower enthalpy levels (<4 MJ/kg), the enthalpy-probe data also agreed well with the bulk calorimeter values. These results indicate that the gas flow down the tunnel center line was adiabatic. However, the enthalpy-probe data were less than the bulk calorimeter data at the higher enthalpies (>4 MJ/kg). Thus it appears, flow kinetics only being considered, that all the energy frozen in the low-density flow entering the probe may not have been sensed. The conclusions regarding the performance of the local total enthalpy probe are weakened somewhat by the lack of a direct comparison standard in the free stream; however, the need for further research on the internal fluid mechanics and chemical kinetics of the flow in such probes in low-density nonequilibrium environments is evident.

The following recommendations are pertinent to the improved performance of this shock-swallowing, self-aspirating enthalpy probe in a low-density nonequilibrium airstream: (1) This design, with the air gap extending to the tip, should not be used as a mass flow probe; (2) probe diameter and length should be made as small as possible to decrease probe response time while maintaining probe accuracy; (3) the mass flow metering section should be isolated from the calorimetric portion of the probe to reduce time response and to exclude extraneous heat sources and/or sinks; (4) mass flow rate calibrations using air heated to temperatures expected during the tests would lend still more confidence to the probe measurements of enthalpy; and (5) a knowledge of the chemistry of the exiting flow is needed and, in this regard, determination of the catalytic efficiency of the air-out thermocouple surface would be helpful.

Langley Research Center,
National Aeronautics and Space Administration,
Hampton, Va., June 27, 1972.

REFERENCES

1. Moffat, Robert J.: Gas Temperature Measurement. Temperature – Its Measurement and Control in Science and Industry, Vol. 3, Pt. 2, Charles M. Herzfeld and A. I. Dahl, eds., Reinhold Pub. Corp., c.1962, pp. 553-571.

2. Boatright, William B.; Stewart, Roger B.; and Grimaud, John E.: Description and Preliminary Calibration Tests of a Small Arc-Heated Hypersonic Wind Tunnel. NASA TN D-1377, 1962.

3. Folck, James L.; and Smith, Richard T.: Calibration of the AFFDL 50 Megawatt Arc Heated Hypersonic Wind Tunnel With a Two-Foot Nozzle. AFFDL-TR-69-36, U.S. Air Force, Aug. 1969.

4. Jorgenson, Leland H.: The Total Enthalpy of a One-Dimensional Nozzle Flow With Various Gases. NASA TN D-2233, 1964.

5. Winovich, Warren: On the Equilibrium Sonic-Flow Method for Evaluating Electric-Arc Air-Heater Performance. NASA TN D-2132, 1964.

6. Pope, Ronald B.: Measurements of Enthalpy in Low-Density Arc-Heated Flows. AIAA J., vol. 6, no. 1, Jan. 1968, pp. 103-110.

7. Arney, G. D., Jr.; and Boylan, D. E.: A Calorimetric Investigation of Some Problems Associated With a Low-Density Hypervelocity Wind Tunnel. AEDC-TDR-63-19 (Contract No. AF 40(600)-1000), Arnold Eng. Dev. Center, Feb. 1963.

8. Guy, Robert W.: A Calibration and Diagnosis of the Test Stream of an Electric Arc-Heated Wind Tunnel. M.A.E. Thesis, Univ. of Virginia, Sept. 1969.

9. Warshawsky, I.; and Kuhns, P. W.: Review of Pneumatic-Probe Thermometer. Temperature – Its Measurement and Control in Science and Industry, Vol. 3, Pt. 2, Charles M. Herzfeld and A. I. Dahl, eds., Reinhold Pub. Corp., c.1962, pp. 573-586.

10. Duckett, Roy J.; and Sebacher, Daniel I.: Velocity Measurements in the Langley 1-Foot (0.305-Meter) Hypersonic Arc Tunnel. NASA TN D-3308, 1966.

11. Incropera, Frank P.; and Leppert, George: Investigation of Arc Jet Temperature-Measurement Techniques. ISA Trans., vol. 6, no. 1, Jan. 1967, pp. 35-41.

12. Grey, Jerry; Jacobs, Paul F.; and Sherman, Martin P.: Calorimetric Probe for the Measurement of Extremely High Temperatures. Rev. Sci. Instrum., vol. 33, no. 7, July 1962, pp. 735-741.

13. Fingerson, L. M.: Research on the Development and Evaluation of a Two Sensor Enthalpy Probe. ARL-64-161 (Contract AF 33(657)-9917), U.S. Air Force, Oct. 1964. (Available from DDC as AD 608 605.)

14. Adams, Donald E.: An Evaporative Film Calorimetric Enthalpy Probe. ARL-65-47 (Contract AF 33(657)-7774), U.S. Air Force, Mar. 1965. (Available from DDC as AD 615 461.)

15. Vassallo, F. A.: High Speed Miniature Enthalpy Probe Development. ARL 70-0018 (Contract No. F33615-69-C-1037), U.S. Air Force, Feb. 1970.

16. Esker, Donald: A Probe for Total Enthalpy Measurements in Arcjet Exhausts. AIAA J., vol. 5, no. 8, Aug. 1967, pp. 1504-1506.

17. Anderson, Lewis A.; and Sheldahl, Robert E.: Flow-Swallowing Enthalpy Probes in Low-Density Plasma Streams. AIAA Paper No. 68-390, Apr. 1968.

18. O'Connor, T. J.; and Comfort, E. H.: Enthalpy-Mass Flux-Impact Pressure Probe System. AFFDL-TR-68-137, U.S. Air Force, Dec. 1968.

19. Boatright, W. B.; Sebacher, D. I.; Guy, R. W.; and Duckett, R. J.: Review of Testing Techniques and Flow Calibration Results for Hypersonic Arc Tunnels. AIAA Paper No. 68-379, Apr. 1968.

20. Grey, Jerry: Thermodynamic Methods of High-Temperature Measurement. ISA Trans., vol. 4, no. 2, Apr. 1965, pp. 102-115.

21. Lordi, J. A.; Mates, R. E.; and Moselle, J. R.: Computer Program for the Numerical Solution of Nonequilibrium Expansions of Reacting Gas Mixtures. Rep. No. AD-1689-A-6 (Contract No. NASr-109), Cornell Aeron. Lab., Inc., Oct. 1965.

22. Eshbach, Ovid W., ed.: Handbook of Engineering Fundamentals. Second ed., John Wiley & Sons, Inc., c.1952.

23. Crites, Roger C.; and Czysz, Paul: Inlet and Test Section Diagnostics Using a Miniature Mass Flow Probe in Hypersonic Impulse Tunnel. AIAA Paper No. 68-389, Apr. 1968.

24. Baird, D. C.: Experimentation: An Introduction to Measurement Theory and Experiment Design. Prentice Hall, Inc., c.1962.

25. Vincenti, Walter G.; and Kruger, Charles H., Jr.: Introduction to Physical Gas Dynamics. John Wiley & Sons, Inc., c.1965.

NASA-Langley, 1972 —— 11 L-8248

"The aeronautical and space activities of the United States shall be conducted so as to contribute . . . to the expansion of human knowledge of phenomena in the atmosphere and space. The Administration shall provide for the widest practicable and appropriate dissemination of information concerning its activities and the results thereof."

—NATIONAL AERONAUTICS AND SPACE ACT OF 1958

NASA SCIENTIFIC AND TECHNICAL PUBLICATIONS

TECHNICAL REPORTS: Scientific and technical information considered important, complete, and a lasting contribution to existing knowledge.

TECHNICAL NOTES: Information less broad in scope but nevertheless of importance as a contribution to existing knowledge.

TECHNICAL MEMORANDUMS: Information receiving limited distribution because of preliminary data, security classification, or other reasons.

CONTRACTOR REPORTS: Scientific and technical information generated under a NASA contract or grant and considered an important contribution to existing knowledge.

TECHNICAL TRANSLATIONS: Information published in a foreign language considered to merit NASA distribution in English.

SPECIAL PUBLICATIONS: Information derived from or of value to NASA activities. Publications include conference proceedings, monographs, data compilations, handbooks, sourcebooks, and special bibliographies.

TECHNOLOGY UTILIZATION PUBLICATIONS: Information on technology used by NASA that may be of particular interest in commercial and other non-aerospace applications. Publications include Tech Briefs, Technology Utilization Reports and Technology Surveys.

Details on the availability of these publications may be obtained from:

SCIENTIFIC AND TECHNICAL INFORMATION OFFICE

NATIONAL AERONAUTICS AND SPACE ADMINISTRATION

Washington, D.C. 20546